Erythrocyte lysis in isotonic solution of ammonium chloride: Theoretical modeling and experimental verification

Andrey V. Chernyshev[a,c,]*, Peter A. Tarasov[a], Konstantin A. Semianov[a],
Vyacheslav M. Nekrasov[a], Alfons G. Hoekstra[b], Valeri P. Maltsev[a,c]

[a]*Institute of Chemical Kinetics and Combustion, Institutskaya 3, Novosibirsk 630090, Russia*
[b]*Faculty of Science, University of Amsterdam, Kruislaan 403, 1098 SJ Amsterdam, The Netherlands*
[c]*Novosibirsk State University, Pirogova 2, Novosibirsk 630090, Russia*

Abstract

A mathematical model of erythrocyte lysis in isotonic solution of ammonium chloride is presented in frames of a statistical approach. The model is used to evaluate several parameters of mature erythrocytes (volume, surface area, hemoglobin concentration, number of anionic exchangers on membrane, elasticity and critical tension of membrane) through their sphering and lysis measured by a scanning flow cytometer (SFC). SFC allows measuring the light-scattering pattern (indicatrix) of an individual cell over the angular range from $10°$ to $60°$. Comparison of the experimentally measured and theoretically calculated light scattering patterns allows discrimination of spherical from non-spherical erythrocytes and evaluation of volume and hemoglobin concentration for individual spherical cells. Three different processes were applied for erythrocytes sphering: (1) colloid osmotic lysis in isotonic solution of ammonium chloride, (2) isovolumetric sphering in the presence of sodium dodecyl sulphate and albumin in neutrally buffered isotonic saline, and (3) osmotic fragility test in hypotonic media. For the hemolysis in ammonium chloride, the evolution of distributions of sphered erythrocytes on volume and hemoglobin content was monitored in real-time experiments. The analysis of experimental data was performed in the context of a statistical approach, taking into account that parameters of erythrocytes vary from cell to cell.
© 2007 Elsevier Ltd. All rights reserved.

Keywords: Mathematical model; Hemolysis; Erythrocyte; Band 3 anionic exchanger; Scanning flow cytometer; Light scattering indicatrix

1. Introduction

Multiparameter assay of erythrocytes, i.e. simultaneous evaluation of their several parameters, such as volume, surface area, hemoglobin concentration, membrane permeability (to some agents), membrane elasticity, membrane critical tension, etc. is carried out applying different methods of erythrocytes treatment. One of the widely used methods is hemolysis in a proper media. A typical native mature erythrocyte has a biconcave discoid shape. In normal conditions, it maintains its volume, ionic composition, pH and membrane structure and integrity. When an erythrocyte is placed in a hemolytic medium, it becomes unstable, and its volume changes. If the hemolysis is of colloid-osmotic type, the cell swells and eventually lyses when the volume exceeds a critical level. The lysis observed in a large population of cells follows an S-shaped relation with time, reflecting the time-course of cell volume, the relation between volume and lysis, and the distribution of cell properties in the population. The capacity of erythrocytes to resist hemolysis can be modified by various pathologies and by a wide variety of physical, chemical or pharmacological treatments. Its study can thus yield relevant information to hematologists and clinicians for diagnostic purposes or fundamental researches.

Detailed kinetic models of hemolysis contain several elements. The first is a description of net ion fluxes, the second cell volume as a function of solute content and the third a relation between cell volume and lysis. There is

*Corresponding author. Institute of Chemical Kinetics and Combustion, Institutskaya 3, Novosibirsk 630090, Russia. Tel.: +7 383 3333240; fax: +7 383 3307350.

E-mail address: andreychernyshev@list.ru (A.V. Chernyshev).

much information and substantial agreement about many aspects of red cell metabolism, membrane transport, pH control and volume regulation (Falke et al., 1985; Freedman and Hoffman, 1979; Galanter et al., 1993; Joshi and Palsson, 1990; Lew and Bookchin, 1986; Motais et al., 1991; Raftos et al., 1990; Werner and Heinrich, 1985). The non-ideal osmotic behavior of hemoglobin, the change in the net charge on impermeant cell ions with pH, and the kinetics and turnover rates of main monovalent ions transporters are all now well characterized, though in different, often incomparable experimental conditions. Following these models, the physiological properties of erythrocytes can be derived from kinetic volume changes (Widdas and Baker, 1998). The last stage of hemolysis, the rupture of the erythrocyte membrane, can be modeled as a spontaneous process by a causal sequence of two thermally activated transitions (Evans et al., 2003; Hategan et al., 2003) resulting in the dependence of the membrane breakage rate on the membrane tension.

A widely used hemolysing agent is ammonia chloride in a proper buffer solution (Motais et al., 1991; Saas, 1979). The first observation regarding the high permeability of erythrocytes to ammonia was made by Hedin (1897), when he found that erythrocytes suspended in isotonic NH_4Cl solution rapidly hemolysed. Later, Jacobs (1924) proposed that the membrane is impermeable to NH_4^+ and the hemolysis is due to diffusion of free NH_3 across the membrane. Once inside the cell, a new equilibrium between NH_3 and NH_4^+ is established and the intracellular OH^- exchanges to the extracellular Cl^- resulting in a net influx of NH_4Cl. Later, it was observed that the transport of OH^- is largely mediated by CO_2/HCO_3^- exchange, so that inhibition of carbonic anhydrase or depletion of CO_2 slows the lysis. Thus, the operation of the Jacobs–Stewart cycle (Jacobs and Stewart, 1942) was established to be a significant factor of red cells swelling in the presence of NH_4Cl. The colloid osmotic hemolysis had subsequently been used to study the permeability of erythrocytes to a variety of organic and inorganic anions by measuring the rate of lysis of erythrocytes suspended in isotonic ammonium salt solutions with the anion of interest. In the presence of CO_2 the rate of hemolysis was observed to be proportional to the rate of influx of the anion, provided that the NH_3 permeability is not rate limiting. Nowadays, it is established that the rate-limiting factor of the hemolysis in isotonic NH_4Cl under typical conditions (in the presence of HCO_3^-) is the Cl^-/HCO_3^- transmembrane exchange through Band 3 anion channel. Therefore, study of hemolysis in isotonic ammonium chloride solution may lead to the evaluation of the amount of Band 3 exchangers on the erythrocyte membrane.

The study of hemolysis is limited by the difficulties of experimental monitoring of red cells parameters (volume, shape, pH, etc.) during the process studied in a population of cells. Even the volume of erythrocyte is a difficult parameter to measure accurately by any method. This difficulty arises partly from the cell shape and its ability to

tumble and deform when transported by flow at moderate velocities. A promising technique that can be used for measurement of morphological parameters of single cells is scanning flow cytometry (SFC) (Maltsev, 2000; Maltsev and Semyanov, 2004; Semianov et al., 2004; Shvalov et al., 1999, 2000). The advantage of SFC is based on the measurement of the angular dependency of light scattered by an individual particle, i.e. its light scattering pattern (indicatrix). The indicatrix is very sensitive to size, refractive index, shape and morphological structure of the particle. The SFC technology provides more detailed information as compared to ordinary flow cytometry, since the light scattering pattern brings much more information than the integrated intensities of light scattered in forward and side angular ranges. The SFC has demonstrated its advantage in non-calibrated real-time measurements of the optical parameters (size and refractive index) of homogeneous spherical particles. Thus, the SFC can be used for the measurement of volumes and hemoglobin concentration of sphered erythrocytes. The later is possible as hemoglobin concentration is correlated to refractive index. However, the application of the SFC for the study of hemolysis is complicated by the fact that sphered erythrocytes are only a fraction of all red cells in the sample at any given time-point of the process.

In the present work, we follow a strategy based on recognition of spherical erythrocytes during hemolysis. First we established theoretically and supported experimentally that the differentiation between spherical and non-spherical erythrocytes is possible on the basis of the Fourier spectrum of light scattering indicatrices. Following this approach, the SFC has been applied for the measurement of partial distributions of sphered erythrocytes on their volume and hemoglobin concentration during hemolysis. The dynamics of colloid-osmotic hemolysis has been monitored in isotonic buffer solutions of the ammonium chloride. A mathematical model was developed to describe the evolution of the sphered erythrocytes distributions during hemolysis. The model has been used for the analysis of the corresponding experimental data in order to obtain dynamic parameters of the erythrocytes. Initial overall distributions of erythrocytes on volume and hemoglobin concentration have been determined in additional experiments measuring spherical red cells prepared by isovolumetric sphering (Kim and Ornstein, 1983). A conventional osmotic fragility test (Delano, 1995; Mazeron et al., 2000) in hypotonic external media was carried out, in order to obtain initial distribution of erythrocytes on the asphericity index.

2. Materials and methods

2.1. Instrumentation

For the study we used a SFC which was described in detail elsewhere (Maltsev, 2000; Maltsev and Semyanov, 2004). The main differences between the SFC and ordinary

flow cytometers are as follows: (1) the laser beam (we used in this study He–Ne laser, 632 nm, 10 mW, Melles-Griot) is coaxial with the flow and (2) the optical system allows the measurement of the light-scattering pattern (indicatrix) from an individual particle. The SFC allows measurements of indicatrices at polar angle ranging from 5° to 100° with integration over the azimuthal angle from 0° to 360°. The SCF angular resolution is equal to the light collection polar angle, which is dependent on the light scattering polar angle. The SFC maximum light collection angle in our experiments was 2° at 40° of the light scattering angle (i.e. for other angles the light collection angle was less then 2°). The dependence of the angular resolution on the light scattering angle was taken into account for interpretation of measured indicatrices, since the increase of the light collection angle leads to the decrease of the indicatrix contrast. Accurate measurement of light scattering indicatrices was available with the rate up to 300 particles per second.

2.2. Sample preparation

Whole blood was taken from a healthy volunteer (27 yr old male) by venopuncture with EDTA as anticoagulant and resuspended in buffered saline (0.01 M HEPES buffer from Sigma, pH 7.4, 0.15 M NaCl). Then the cells were used in experiments at room temperature (20 °C) within 3 h. All blood samples were taken from the same donor.

2.3. Hemolysis with ammonium chloride

Volume containing 5 μl of blood was placed into a testing tube with 1 ml of the lysing solution to achieve an initial concentration in the range from 0.5×10^7 to 2×10^7 cells per milliliter. As lysing solution we used an isotonic (0.15 M) concentration of ammonium chloride (NH_4Cl) in degassed (boiled for 10 min) water solution with 1.5 mM buffer HEPES (Sigma) and known (in the range from 1 to 2 mM) concentration of sodium bicarbonate ($NaHCO_3$). The solution provided a constant pH = 7.2 in the external media during hemolysis that was verified independently. The solution was prepared prior to experiments and used within an hour. To ensure homogeneity of the cell suspension the sample was stirred up by pipetting. The overall delay for sample preparation (before measurements) was about 15 s. Then the testing tube was attached to the SFC to provide real-time measurements of the cells during hemolysis. During the course of experiment the sample was under gentle agitation.

2.4. Isovolumetric sphering procedure

Isovolumetric sphering (Kim and Ornstein, 1983) of the erythrocytes is done in the presence of sodium dodecyl sulphate (SDS) and albumin in neutrally buffered isotonic saline. A close to ideal sphering is achieved by balancing the weight ratio of SDS/protein at approximately 1/50 or

less. The use of endogenous serum protein is possible: a dilution of whole blood of 1/50 in phosphate buffer saline with 0.003% SDS for a minute and consequent dilution of 1/25 by isotonic saline of 0.1% glutaraldehyde and 0.001% SDS. We followed the modification of this method where 0.1% of human serum albumin is presented in the surrounding isotonic medium as a protecting agent and SDS concentration is 0.004%.

2.5. Osmotic fragility test

The conventional osmotic fragility test (Delano, 1995; Mazeron et al., 2000) was performed placing an aliquot of a stock solution of blood into a series of phosphate buffered saline (PBS) solutions of decreased osmotic pressure with consequent calculation a percent of hemolysed cells.

3. Theoretical modeling

3.1. Recognition of spherical erythrocytes

It is generally believed that in the ultimate stage of swelling, an erythrocyte approaches an oblate spheroid shape before it becomes spherical. The assumption was supported by theoretical considerations and experimental observations (Fisher et al., 1981). Based on this assumption a T-matrix method (Mishchenko and Travis, 1994) for spheroids was applied for theoretical modeling of light-scattering indicatrices of swollen erythrocytes. For the calculations we used known data on complex refractive index (Faber et al., 2004) of hemoglobin, as well as the range of volumes (Kim and Ornstein, 1983) and hemoglobin concentrations (Raftos et al., 1990) of human erythrocytes. Our method to recognize sphered erythrocytes is based on a spectral decomposition approach (Semianov et al., 2004). The essence of this method is the Fourier spectrum analysis of a modified light scattering indicatrix, $F(\theta)$. The modification of the original indicatrix, $I(\theta)$, to the function $F(\theta)$ is done by the standard Hanning window procedure:

$$F(\theta) = I(\theta)f(\theta) = I(\theta)\sin^2\left(\pi\frac{\theta - \theta_l}{\theta_h - \theta_l}\right),\qquad(1)$$

where $\theta_l = 10°$ и $\theta_h = 50°$ are the lowest and highest angles of the angular range of the indicatrix. We define the "asphericity index" δ_c as the ratio of surface-area-equivalent sphere volume, V_{cs}, to the spheroid volume, V_c. We have computed modified indicatrices for spheroids as a function of the asphericity index for volumes and refractive indices representing human erythrocytes. As demonstrated in Fig. 1, the maximum peak amplitude A_f of the normalized Fourier spectrum (i.e. the Fourier amplitude spectrum divided by the zero frequency peak amplitude) of the modified indicatrix $F(\theta)$ depends on the asphericity index of the spheroid. Fig. 2 shows results of theoretical calculations of A_f varying morphological
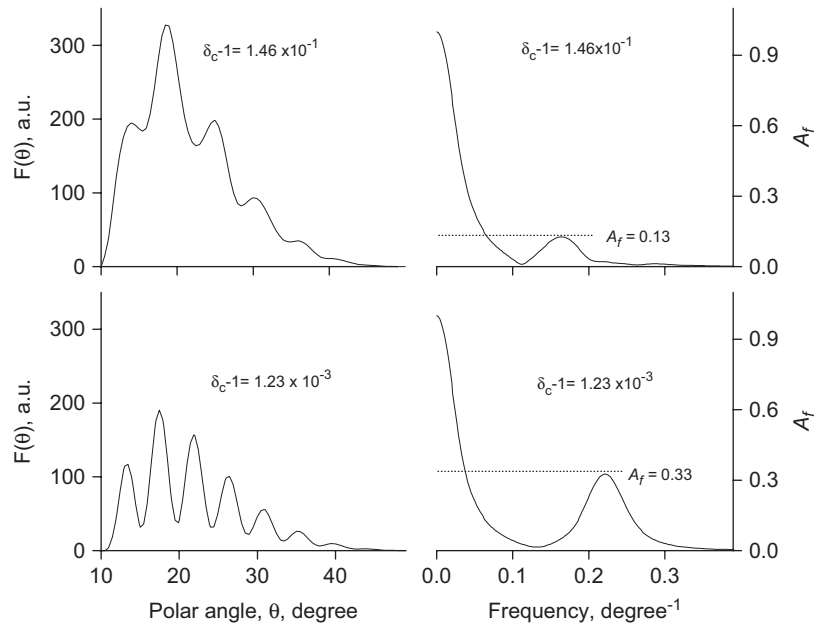
Fig. 1. Modified theoretical indicatrices, $F(\theta)$, (left pictures) and corresponding normalized amplitude FFT spectra (right pictures) at different asphericity index δ_c of an oblate spheroid. The surface area and the hemoglobin content of the spheroid are $130\,\mu m^2$ and $400\,mM\,\mu m^3$, respectively. The angle β between the spheroid axis of symmetry and the incident laser beam is $90°$.
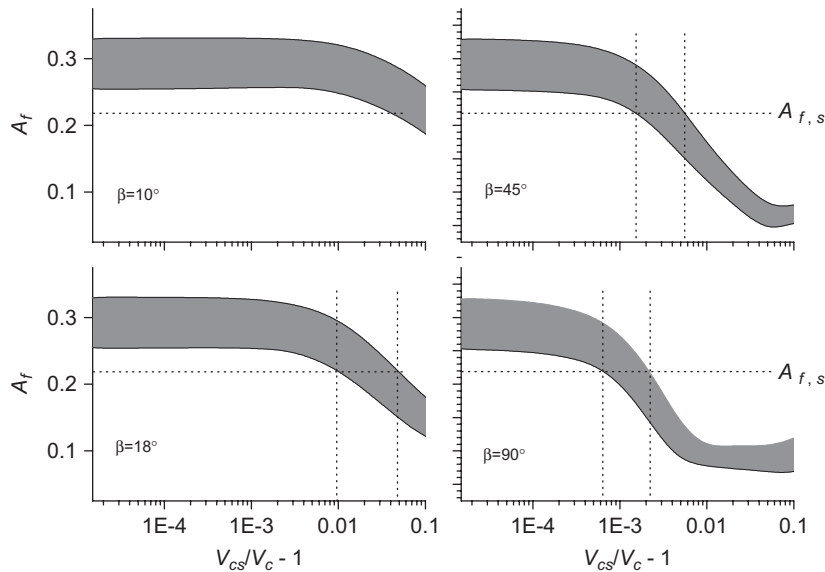

Fig. 2. Theoretical calculations of the dependency of the Fourier parameter A_f on the asphericity index δ_c of an oblate spheroid during the process of increasing of volume with conservation of surface area and hemoglobin content under the following conditions: surface area is in the range from 110 to $160\,\mu m^2$; hemoglobin content is in the range from 300 to $600\,mM\,\mu m^3$. The dependence of the angular resolution on the light scattering angle was taken into account, assuming that the SFC maximum light collection angle was $2°$ at $40°$ of light scattering angle. Four pictures correspond to different orientation of the oblate spheroid, and β is the angle between the spheroid axis of symmetry and the incident laser beam.

parameters and orientation of an erythrocyte. For the calculations, the dependence (Maltsev, 2000) of the SFC angular resolution on the light scattering angle was taken into account, since the increase of the light collection angle leads to the decrease of the indicatrix contrast (and, therefore, to the decrease of A_f). The "key point" of the recognition method is that A_f is increasing sharply in a narrow range of the asphericity index when a spheroid

approaches the spherical shape (see Fig. 2). We call this the critical range. In that range the asphericity index is very close to unity. Therefore, it is convenient to use the "relative asphericity index", which is $(V_{cs} - V_c)/V_c = \delta_c - 1$. According to the data shown in Fig. 2, the "critical relative asphericity index" range (marked by two vertical dashed lines) depends on the orientation of the spheroid to the direction of the incident light (angle β) and corresponds

to some "critical peak amplitude" A_f (marked by a horizontal dashed line). If one selects, for example, a critical $A_f = 0.22$, it corresponds to the following critical "relative asphericity indexes" at different angles β: $(0.6–2.2) \times 10^{-3}$ at $\beta = 90°$; $(1.5–5.5) \times 10^{-3}$ at $\beta = 45°$; $(0.9–4.8) \times 10^{-2}$ at $\beta = 18°$. Thus, we used the following recognition method in our measurements: an erythrocyte is considered to have a spherical shape (approximately), if its A_f exceeds a critical level of 0.22. Assuming random orientation of swollen erythrocytes, the partial amount of cells with the angle β in the range from 0° to 18°, $N(\beta < 18°)$, of the total amount N_0 is estimated as

$$\frac{N(\beta < 18°)}{N_0} = \int_0^{18°} \sin(\theta)\mathrm{d}\theta \approx 0.049, \tag{2}$$

i.e. less than 5% of cells have $\beta < 10°$. Therefore, if one neglects 5% of all erythrocytes, the vale of 0.22 for A_f can be used to separate the cells with relative asphericity index less than 0.05. In a real case, one should neglect even less than 5% of all erythrocytes due to a bell-like shape of distributions of erythrocytes on their parameters.

As soon as a cell is recognized as being spherical, the parametric solution of the inverse light scattering problem for spheres can be applied for determination of the size and refractive index and, consequently, the volume and hemoglobin content of the cell (Shvalov et al., 1999). The algorithm is applicable in ranges of spherical cell volume of 20–300 μm^3 and hemoglobin concentration of 1–6.6 mM.

3.2. Mathematical model of osmotic fragility test

In the osmotic fragility test, an aliquot of a stock solution of blood is placed into a series of PBS solutions where the osmotic pressure is decreased (compared to the condition when erythrocytes have their native volume and intracellular solutes concentration) by reduction of the PBS concentration. Due to equilibration of the osmotic pressure over an erythrocyte membrane, the cell swells up to some extent. If the erythrocyte cannot equilibrate the osmotic pressure by the swelling, hemolysis of the cell occurs. Since erythrocytes vary from each other on their individual parameters, the hemolysis observed in a large population of cells follows an S-shaped curve with PBS concentration. The balance of the extracellular and the intracellular osmotic pressures can be represented as

$$\sum_i C_{iw} + \phi_{Hb}[Hb]_w = [PBS]_w, \tag{3}$$

where the square brackets denote the concentration of hemoglobin, Hb, or PBS; the subscript "w" means that the concentration is relative to the water volume of the media; the summation on i is taken over the concentrations C_{wi} of all intracellular solutes other then hemoglobin; ϕ_{Hb} is the osmotic coefficient of hemoglobin (Freedman and Hoffman, 1979):

$$\phi_{Hb} = 1 + 0.0645[Hb]_w + 0.0258[Hb]_w^2. \tag{4}$$

In Eq. (4) the concentration of hemoglobin is taken in millimole/liter (mM) units. It is assumed in Eq. (3), that the osmotic coefficient of solutes other than hemoglobin is unity. The difference between the total volume and the water volume may be significant in the case of the presence of the molecules with high molecular weight in the medium. For example, due to the presence of hemoglobin typical erythrocyte water content (Raftos et al., 1990) is about 0.717 (i.e. the cell water volume is about 28% less than its total volume). We used the following equation for the relation between the intracellular concentrations:

$$C_{iw} = \frac{C_{ic}}{1 - [Hb]_c v_{Hb}}, \tag{5}$$

where the subscript "c" means that the concentration C_i of the i-compound is relative to the cell volume; $[Hb]_c$ is the hemoglobin concentration relative to the cell volume; $v_{Hb} = 48.3$ liter/mol (Cameron and Fullerton, 1990) is the molar volume of hemoglobin. In Eq. (5) we assumed that the volume hindered from water molecules by hemoglobin is proportional to the number of hemoglobin molecules in the medium. In the extracellular media there is no significant difference between water volume and total volume.

During swelling a red cell contains the same molar amount of intracellular solutes, therefore Eq. (3) leads to a relation between the PBS concentration and the cell water volume V_w:

$$[PBS]_{w0}V_{w0} - \phi_{Hb0}[Hb]_{w0}V_{w0} = [PBS]_w V_w - \phi_{Hb}[Hb]_w V_w, \tag{6}$$

where subscript "0" means the values under conditions where an erythrocyte has its native volume V_{w0} and hemoglobin concentration $[Hb]_{w0}$. The relative volume expansion α can be expressed either through cell water volumes, $\alpha_w = V_w/V_{w0}$, or total cell volumes, $\alpha_c = V_c/V_{c0}$. The relation between α_w and α_c follows from Eq. (5):

$$\alpha_w = \frac{\alpha_c - [Hb]_{c0}v_{Hb}}{1 - [Hb]_{c0}v_{Hb}}. \tag{7}$$

An erythrocyte is hemolysed, if its relative volume expansion α_c exceeds the asphericity index of the erythrocyte $\delta_c = V_{cs}/V_{c0}$. Thus, the critical PBS concentration can be calculated for an individual erythrocyte substituting its values of δ_c, V_{w0}, and $[Hb]_{w0}$ into Eq. (6). In a large population of cells, the S-shaped relation between the amount of hemolysed cells and PBS concentration is calculated taking into account distributions of the cells on their individual parameters δ_c, V_{w0}, and $[Hb]_{w0}$.

3.3. Mathematical model of hemolysis in isotonic solution of ammonium chloride

In the model, the extracellular conditions (pH, reagents concentrations, temperature, etc.) are considered to be unchanged during hemolysis. In the water solution, NH_4Cl is presented in the form of the ions NH_4^+ and Cl^-, while NH_4^+ is partially dissociated in NH_3 and H^+:

$$NH_4^+ \leftrightarrow NH_3 + H^+. \tag{8}$$
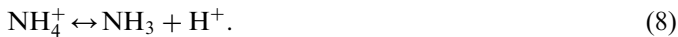
The equilibrium constant of reaction (8) is $10^{-9.25}$ M, therefore the concentration of NH_3 equals

$$[NH_3]_w = \frac{K_1[NH_4^+]_w}{[H^+]_w} = [NH_4^+]_w \times 10^{pH-9.25}. \tag{9}$$

Therefore, in an isotonic solution of ammonium chloride (150 mM of NH_4^+) at a typical pH of 7.2 the concentration of NH_3 is about 1.5 mM. The red cell membrane is poorly permeable to NH_4^+, as to other cations, but highly permeable to uncharged NH_3. The value of 0.21 cm/s (Labotka et al., 1995) for NH_3 permeability of erythrocyte membrane indicates that the equilibration of extracellular and intracellular concentrations of NH_3 is reached within $\sim 10^{-3}$ s. Even for unstirred samples (the permeability for unstirred layers is about 1.1×10^{-3} cm/s (Labotka et al., 1995) the NH_3 transmembrane equalization is reached within ~ 0.2 s. Under conditions used in this study, the time of hemolysis was ~ 100 s. Therefore, a transmembrane equilibrium for NH_3 existed for most time during hemolysis. In other words, we assume

$$[NH_3(ex)]_w = [NH_3(in)]_w, \tag{10}$$

where "*ex*" and "*in*" in round brackets denote extracellular and intracellular locations of the compound, correspondingly. On the other hand, due to the time scale of ~ 100 s, one can neglect much slower process of the transport ammonia through NH_4^+/H^+ exchangers (Rh-glycoproteins).

Theoretically, the process of hemolysis in isotonic solutions of NH_4Cl was divided into three successive stages: (1) initial penetration of NH_3 leading to transmembrane equilibration of the NH_3 concentration (in less than 0.2 s); (2) erythrocyte swelling to its spherical shape (much longer than 0.2 s); (3) rupture of the membrane and cell decay (much longer than 0.2 s). The classification is useful, since the rate-limiting factor changes from stage to stage. An important question is how the erythrocyte intracellular pH changes during cell volume expansion in each stage. We used known data (Raftos et al., 1990) on the electrochemical model of erythrocyte buffering (dissociation constants and the range of typical concentrations of main solutes, see Table 1), taking into account that the total concentration of extracellular and intracellular carbonates (CO_2, H_2CO_3, HCO_3^-, CO_3^{2-}) is controlled by adding known concentration of $NaHCO_3$ (in the range from 1 to 2 mM) to the degassed water solution.

In water solution, $NaHCO_3$ is present in the form of the ions Na^+ and HCO_3^-, and the anion HCO_3^- is involved in a set of reversible dissociation–association and hydration–dehydration reactions which control the concentration of other carbonates (CO_2, H_2CO_3, and CO_3^{2-}):

$$HCO_3^- + H^+ \leftrightarrow H_2CO_3, \tag{11}$$

$$HCO_3^- \leftrightarrow CO_3^{2-} + H^+, \tag{12}$$

$$H_2CO_3 \leftrightarrow H_2O + CO_2. \tag{13}$$

Reactions (11) and (12) reach equilibrium rather fast both inside and outside the cell (within < 1 ms). In pure water the forward and backward rate constants for reaction (13) at 25 °C are $12\,s^{-1}$ and $3 \times 10^{-2}\,s^{-1}$, respectively (Dreybrodt et al., 1996), yielding a rate constant of equilibration of $\sim 12\,s^{-1}$. Inside the erythrocyte reaction (13) occurs much faster due to the presence of carbonic anhydrase. Thus, the equilibration for the set of reactions (11)–(13) is reached within < 1 s. At equilibrium, the concentration of a certain carbonate can be expressed through the concentration of the dissolved carbon dioxide (Raftos et al., 1990) as

$$\left\lfloor HCO_3^- \right\rfloor_w = [CO_2]_w \times 10^{pH-6.11}, \tag{14}$$

$$\left\lfloor CO_3^{2-} \right\rfloor_w = [CO_2]_w \times 10^{2pH-16.31}. \tag{15}$$

Table 1

Concentrations (relative to water volume), charge terms, and dissociation constants for the intracellular solutes used for modeling (carbonates are not included)[a]

Solute	Concentration range[b] mM	Apparent pK_a	Proton charge per molecule[c]
Hemoglobin	6.3–7.4	6.69; 7.89	$z_{Hb} = 15.6 - 23b_1/(1+b_1) - 4b_2/(1+b_2)$
DPG	5.4–10.7	7.56; 7.32	$z_{DPG} = -3 - b_1/(1+b_1) - b_2/(1+b_2)$
ATP	1.3–3.4	6.80	$z_{ATP} = -3 - b/(1+b)$
GSH	2.7–3.5	8.54; 9.42	$z_{DPG} = -1 - b_1/(1+b_1) - b_2/(1+b_2)$
Pi[d]	0.4–1.4	6.87	$z_{Pi} = -1 - b/(1+b)$
Cl	61–73	–	$z_{Cl} = -1$

[a]The data were taken from the paper of Raftos et al. (1990).
[b]The concentrations related to water volume were obtained applying Eq. (5) for the corresponding data.
[c]For a particular solute: $b = 10^{pH-pK_a}$ or $b_1 = 10^{pH-pK_{a1}}$ and $b_2 = 10^{pH-pK_{a2}}$.
[d]The range for this solute was estimated as 50% of its average value.

The equilibrium concentration of H_2CO_3 at 25 °C can be evaluated as (Dreybrodt et al., 1996)

$$[H_2CO_3]_w = [CO_2]_w \times 10^{-2.60}. \tag{16}$$

The total concentration of external carbonates is equal to the concentration of added $NaHCO_3$:

$$[CO_2(ex)]_w + [H_2CO_3(ex)]_w + [HCO_3^-(ex)]_w$$
$$+ [CO_3^{2-}(ex)]_w = [NaHCO_3]_{added}. \tag{17}$$

Using Eqs. (14)–(17) one can find the concentration of dissolved carbon dioxide as:

$$[CO_2(ex)]_w = \frac{[NaHCO_3]_{added}}{1 + 10^{-2.60} + 10^{pH_{ex}-6.11} + 10^{2pH_{ex}-16.31}}. \tag{18}$$

The permeability of carbon dioxide through the erythrocyte membrane (~ 0.58 cm/s; (Klocke, 1988)) is rather close to the permeability of NH_3 for unstirred layers (~ 0.21 cm/s; (Labotka et al., 1995)). Therefore, the transmembrane equilibrium for CO_2,

$$[CO_2(ex)]_w = [CO_2(in)]_w \tag{19}$$

is reached during the first stage of hemolysis at about the same rate as the transmembrane equilibrium for NH_3.

Thus, during the first stage, the only solutes whose penetration is taken into account are NH_3 and CO_2, resulting in equilibration of their intracellular and extracellular concentrations at the end of the first stage. The effect of CO_2 on buffer properties of the medium is taken into account by evaluating the negative charge due to the total carbonates Q_c through the concentration of dissolved CO_2 and the effective charge z_c (as function of intracellular pH), as it follows from Eqs. (14) and (15):

$$Q_c = -(\lfloor HCO_3^- \rfloor + 2 \lfloor CO_s^{2-} \rfloor))V_w = z_c(pH)[CO_2(in)]V_w, \tag{20}$$

where

$$z_c(pH) = 10^{pH-6.11} + 2 \times 10^{2pH-16.31}. \tag{21}$$

Then the equation describing conservation of total charge of the cell during the first stage is:

$$[NH_4^+(in)]_w V_w + z_c(pH_{in})[CO_2(in)]_w V_w$$
$$- z_c(pH_{in0})[CO_2(in)]_{w0} V_{w0}$$
$$+ \sum_i (z_i(pH_{in}) - z_i(pH_{in0}))P_i = 0, \tag{22}$$

where the subscript "0" denotes the value at initial conditions (before penetration of NH_3); pH_{in} is the intracellular pH; z_i (as function of pH) is the charge of

one mole of the intracellular i-compound, other than carbonates and NH_4^+; and P_i is the number of moles of the intracellular i-compound, which is considered to be constant during the first stage (i.e. the compound other than carbonates and NH_4^+):

$$P_i = C_{iw0} V_{w0} = C_{iw} V_w. \tag{23}$$

Taking into account Eqs. (10) and (19), Eq. (22) can be rewritten as

$$\frac{V_w}{V_{w0}} = - \frac{\sum_i (z_i(pH_{in}) - z_i(pH_{in0}))C_{iw0}}{[NH_4^+(ex)]_w \times 10^{pH_{ex}-pH_{in}} + z_c(pH_{in})[CO_2(ex)]_w - z_c(pH_{in0})[CO_2(in)]_{w0}}, \tag{24}$$

where the extracellular pH_{ex} and $[NH_4^+(ex)]_w$ are constants during the process. Using Eq. (24) one can calculate the relative change of the cell water volume for a given intacellular pH_{in} which is reached during the first stage of the hemolysis in the presence of extracellular NH_4^+. On the other hand, the solution of Eq. (24) should correspond to equality of the extracellular and the intracellular osmotic pressures:

$$\sum_j (\phi_j C_{jw} - \phi_{j0} C_{jw0}) = 0, \tag{25}$$

where ϕ_j is the osmotic coefficient of the intracellular j-compound. The summation in Eq. (25) is taken over all intracellular compounds. The dependence of the osmotic coefficient on the concentration is assumed only for hemoglobin (Eq. (4)). For solutes other than hemoglobin the osmotic coefficient is assumed equal to unity. Using Eqs. (9) and (10), Eq. (25) can be represented as

$$[NH_4^+(ex)]_w \cdot (10^{pH_{ex}-pH_{in}} + 10^{pH_{ex}-9.25}) + \phi_{Hb}[Hb]_w$$
$$- \phi_{Hb0}[Hb]_{w0} + c_w(in) - c_{w0}(in) + \left(\frac{V_{w0}}{V_w} - 1\right) \sum_i C_{iw0} = 0, \tag{26}$$

where the summation is taken over all intracellular solutes other then ammonia, hemoglobin and carbonates; and c_w is the total concentration of carbonates, which is expressed as:

$$c_w = [CO_2]_w (1 + 10^{-2.60} + 10^{pH-6.11} + 10^{2pH-16.31}). \tag{27}$$

At the start of the first stage of the hemolysis the initial concentrations of intracellular solutes correspond to initial osmotic balance in isotonic solution ($[NH_4^+(ex)]_w = 150$ mM):

$$\phi_{Hb0}[Hb]_{w0} + c_{w0}(in) + \sum_i C_{iw0} = 2[NH_4^+(ex)]_w, \tag{28}$$

where the summation on i is taken over all intracellular solutes other then hemoglobin and carbonates. Substituting the expression for the sum $\sum_i C_{iw0}$ from Eq. (28) into

Eq. (26) we get

$$[NH_4^+(ex)]_w(10^{pH_{ex}-pH_{in}} + 10^{pH_{ex}-9.25}) + \phi_{Hb}[Hb]_w$$

$$- \phi_{Hb0}[Hb]_{w0} + c_w(in) - c_{w0}(in) + \left(\frac{V_{w0}}{V_w} - 1\right)$$

$$\times (2[NH_4^+(ex)]_w - \phi_{Hb0}[Hb]_{w0} - c_{w0}(in)) = 0. \qquad (29)$$

intracellular Cl^- anions via transmembrane exchange of extracellular Cl^- with HCO_3^- intracellular anions. Applying the electrochemical and osmotic model of erythrocyte discussed above, one can estimated the change of pH_{in} and volume of the erythrocyte when adding some amount of Cl^- to the intracellular medium. In this case, Eq. (24) should be modified, as follows

$$\frac{V_w}{V_{w1}} = \frac{(N_{Cl}/V_{w1}) - \sum_i(z_i(pH_{in}) - z_i(pH_{in1}))C_{i1}}{[NH_4^+(ex)] \times 10^{pH_{ex}}(10^{-pH_{in}} - 10^{-pH_{in1}}) + (z_c(pH_{in}) - z_c(pH_{in1}))[CO_2(ex)]} \qquad (32)$$

Substituting the expression for the volume ratio from Eq. (24) into Eq. (29) one obtains the osmotic pressure difference (which is equal to zero) as function of the intracellular pH_{in}. From Eqs. (24) and (29) one can conclude that in order to evaluate the change of the volume and pH_{in} of the erythrocyte during the first stage of the hemolysis one does not have to know concentrations of all intracellular solutes. It is sufficient to know the concentrations of the solutes that change their charge with pH. Typical ranges of the concentrations of such solutes and their charge terms are presented in Table 1.

Thus, the method to compute the volume ratio during the first stage of hemolysis is as follows. First Eqs. (29) and (24) are used to find the value of pH_{in} where the osmotic difference taken equal to zero. Next, Eq. (24) is used to find the volume ratio which corresponds to this value of pH_{in}. Using this procedure and varying the intracellular solutes concentrations over their typical ranges (Table 1) one can find that the dependence of V_{w1}/V_{w0} on the intracellular concentrations other than hemoglobin and $NaHCO_3$ is negligible (less than 2%). Here, subscript "1" denotes the value at the end of the first stage of hemolysis. We found that the dependence of V_{w1}/V_{w0} and pH_{in1} on extracellular $[NaHCO_3]_w$ (from 1 to 8 mM) and intracellular $[Hb]_{w0}$ (from 5 to 8.5 mM) can be approximated (within the error of $\sim$3%) by the expression:

$$\frac{V_{w1}}{V_{w0}} = 1.084 + 0.0238[NaHCO_3]_w + 0.00719[Hb]_w$$

$$- 0.0011[NaHCO_3]_w[Hb]_{w0}, \qquad (30)$$

$$pH_{in1} = 8.049 - 0.263[NaHCO_3]_w - 0.0335[Hb]_{w0}$$

$$+ 0.002[NaHCO_3]_w[Hb]_{w0}. \qquad (31)$$

All concentrations in Eqs. (30) and (31) are in mM units. It is known that a typical erythrocyte reaches its spherical shape when the volume ratio V_{w1}/V_{w0} exceeds 2. It follows from Eq. (30) that at the end of the first stage of hemolysis a typical erythrocyte has not reached its spherical shape yet, while increases slightly the volume.

During the second stage of hemolysis, the rate limiting factor of swelling is the increase of the amount of

and Eq. (29) is changed to

$$[NH_4^+(ex)]_w \times 10^{pH_{ex}}(10^{-pH_{in}} - 10^{-pH_{in1}}) + \phi_{Hb}[Hb]_w$$

$$- \phi_{Hb1}[Hb]_{w1} + c_w(in) - c_{w1}(in) + \left(\frac{V_{w1}}{V_w} - 1\right)$$

$$(2[NH_4^+(ex)]_w - \phi_{Hb1}[Hb]_{w1} - c_{w1}(in)) + \frac{N_{Cl}}{V_{w1}}\frac{V_{w1}}{V_w} = 0,$$

$$(33)$$

where N_{Cl} is the amount of Cl^- anions which were added to intracellular medium during the second stage of hemolysis. With Eqs. (32) and (33) one can find V_w/V_{w1} and pH_{in} at a given N_{Cl}/V_{w1}. Varying the intracellular solutes concentrations over their typical ranges (Table 1), one can find that the dependence of V_w/V_{w1} on the initial intracellular concentrations of the solutes other then hemoglobin is negligible (less than 2%) in the range of N_{Cl}/V_{w1} from 0 to 180 mM. Varying intracellular $[Hb]_{w0}$ (from 5 to 8.5 mM), extracellular $[NaHCO_3]_w$ (from 1 to 8 mM) and N_{Cl}/V_{w1} (from 0 to 180 mM) we found the following approximate expression (within the error of $\sim$3%) for V_w/V_{w1} and pH_{in}:

$$\frac{V_w}{V_{w1}} = 1 + (6.02 - 0.09[NaHCO_3]_w - 0.07[Hb]_{w0})$$

$$\times 10^{-3}\frac{N_{Cl}}{V_{w1}} + (2.1 + 0.184[NaHCO_3]_w$$

$$+ 0.115[Hb]_{w0}) \times 10^{-6}\left(\frac{N_{Cl}}{V_{w1}}\right)^2, \qquad (34)$$

$$pH_{in} = 7.089 + \frac{80 + 0.536[NaHCO_3]_w - 1.75[Hb]_{w0}}{(N_{Cl}/V_{w1}) + 85.4 + 2.6[NaHCO_3]_w + 0.963[Hb]_{w0}}.$$

$$(35)$$

All concentrations in Eqs. (34) and (35) are in mM units. From equation (35) one can see that pH_{in} is decreasing from pH_{in1} to pH_{in2} in the range 7.2–7.9. In the range of N_{Cl}/V_{w1} from 15 to 180 mM the following linear equation fits well the ratio of N_{Cl}/V_{w1}:

$$\frac{N_{Cl}}{V_{w1}} = -165 + (162 + 0.693[NaHCO_3]_w$$

$$+ 0.549[Hb]_{w0})\frac{V_w}{V_{w1}}. \qquad (36)$$

The ratio N_{Cl}/V_{w1} can be expressed through the initial intracellular chlorine concentration $[Cl^-(in)]_{w0}$ and the

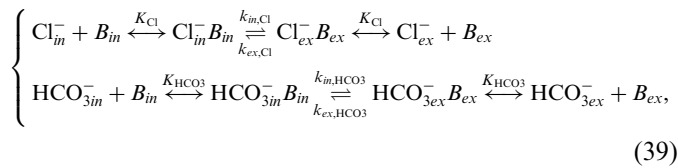current intracellular chlorine concentration $[Cl(in)]_w$:

$$\frac{N_{Cl}}{V_{w1}} = [Cl(in)]_w \frac{V_w}{V_{w1}} - [Cl(in)]_{w0} \frac{V_{w0}}{V_{w1}}. \tag{37}$$

Substituting Eq. (37) into Eq. (36) the equation for $[Cl(in)]_w$ is obtained:

$$[Cl(in)]_w = \frac{V_{w1}}{V_w}\left([Cl(in)]_{w0}\frac{V_{w0}}{V_{w1}} - 165\right) + 162$$
$$+ 0.693[NaHCO_3]_w + 0.549[Hb]_{w0}. \tag{38}$$

It should be noted that the approximation (38) is valid in the range of V_{w1}/V_w from 0.5 to 1 (i.e. V_w/V_{w1} from 1 to 2) corresponding to the range of N_{Cl}/V_{w1} from 0 to 180 mM.

The rate of accumulation of Cl^- by the erythrocyte during the second stage of hemolysis is calculated following a ping-pong model of the Band 3 mediated anion exchange process:

$$\begin{cases} Cl^-_{in} + B_{in} \xleftrightarrow{K_{Cl}} Cl^-_{in}B_{in} \underset{k_{ex,Cl}}{\overset{k_{in,Cl}}{\rightleftharpoons}} Cl^-_{ex}B_{ex} \xleftrightarrow{K_{Cl}} Cl^-_{ex} + B_{ex} \\ HCO^-_{3in} + B_{in} \xleftrightarrow{K_{HCO3}} HCO^-_{3in}B_{in} \underset{k_{ex,HCO3}}{\overset{k_{in,HCO3}}{\rightleftharpoons}} HCO^-_{3ex}B_{ex} \xleftrightarrow{K_{HCO3}} HCO^-_{3ex} + B_{ex}, \end{cases} \tag{39}$$

where B_{ex} and B_{in} are outward- and inward-facing carriers (i.e. Band3 exchangers) on the erythrocyte membrane, correspondingly; and K_{Cl}, K_{HCO3}, $k_{in,Cl}$, $k_{ex,Cl}$, $k_{in,HCO3}$, $k_{ex,HCO3}$ are corresponding Michaelis-Menten constants. By using reaction scheme (39) we took into account the results of Liu et al. (1996), who found that the equilibrium constant of the binding of anions with Band 3 is independent on the carrier facing (i.e., $K_{in,A^-} = K_{ex,A^-} = K_{A^-}$), and that the asymmetry of the anion transport is due to the difference between the translocation rate constants k_{in,A^-} and k_{ex,A^-}. In the reaction scheme (39) we neglected the inhibition of Band 3 by anions Cl^- and HCO_3^-, since typical concentrations of the anions in this study are much smaller then the corresponding inhibition constants. It is well known that the pH dependence of Band 3 anion exchanger follows a roughly bell-shaped curve. The anion exchange rate increases up to pH = 7, then reaches a plateau in the pH range 7–11 and then shows a sharp decrease (Gunn et al., 1973). In our case, pH_{in} is changing in the range from 7 to 8 (see Eq. (35)), therefore, we neglected pH dependence of the Michaelis-Menten constants. Using data from literature (Gasbjerg et al., 1996; Gasbjerg and Brahm, 1991; Knauf et al., 1996), we estimated the values of the Michaelis-Menten constants at $T = 20\,^\circ C$ as follow: $K_{Cl} \approx K_{HCO3} \approx 50\,mM$; $k_{in,Cl} \approx k_{in,HCO3} \approx 8.1 \times 10^3$ ions/s/carrier; $k_{ex,Cl} \approx k_{ex,HCO3} \approx 8.1 \times 10^4$ ions/s/carrier. The rates are expressed in terms of ions per second per carrier using the value of 10^6 carriers/cell (Steck, 1974) and a cell membrane area of $1.42 \times 10^{-6}\,cm^2$ (Knauf et al., 1996). As a result of numerical evaluation of the reaction scheme (39) in the range of extracellular $[NaHCO_3]_w$ from 0.1 to 4 mM, and V_w/V_{w1} from 1.0 to 2.0 for typical concentrations of intracellular $[Hb]_{w0}$ (5–8.5 mM) and $[Cl^-(in)]_{w0}$ (40–90 mM), we

obtained the following approximation (within 5% error) for the net (ingoing) flux of Cl^- through one carrier:

$$j_{Cl}^{in} = [NaHCO_3]\left(G_1 + \frac{G_2}{V_w/V_{w1} + G_3}\right), \tag{40}$$

$$G_1 = -5.883(1 + 0.06347[NaHCO_3] + 0.09077[Hb]_{w0}$$
$$- 0.00261[Cl^-(in)]_{w0}), \tag{41}$$

$$G_2 = 64.55(1 - 0.0041[NaHCO_3] - 0.01643[Hb]_{w0}$$
$$- 0.0032[Cl^-(in)]_{w0}), \tag{42}$$

$$G_3 = -0.9641 + 0.01324[NaHCO_3] + 0.00805[Hb]_{w0}$$
$$+ 0.00097[Cl^-(in)]_{w0}. \tag{43}$$

In Eqs. (40)–(43) the flux j_{Cl}^{in} is in units of ions/s/carrier, and concentrations are in mM.

In order to derive an equation for the relative cell volume V_w/V_{w1} as function of time, the following differential equation is used:

$$\frac{dN_{Cl}}{dt} = J_{Cl}^{in}. \tag{44}$$

Substituting Eqs. (36) and (40) into Eq. (44) one gets

$$\frac{d}{dt}(V_w/V_{w1}) = G_4\left(G_1 + \frac{G_2}{V_w/V_{w1} + G_3}\right), \tag{45}$$

$$G_4 = \frac{[NaHCO_3]B10^{18}}{(162 + 0.693[NaHCO_3] + 0.549[Hb]_{w0})V_{w1}N_a}, \tag{46}$$

where N_a is Avogadro's number, B is the number of carriers, V_{w1} is in μm^3. The solution of the Eq. (45) can be presented as

$$\frac{V_w}{V_{w1}} - 1 - \frac{G_2}{G_1}\ln\left(1 + \frac{(V_w/V_{w1}) - 1}{1 + G_3 + (G_2/G_1)}\right) = G_4G_1t. \tag{47}$$

Therefore, the time of swelling t_2 (until the erythrocyte reached its spherical shape) is:

$$t_2 = \frac{1}{G_1G_4}\left(\frac{V_{w2}}{V_{w1}} - 1 - \frac{G_2}{G_1}\ln\left(1 + \frac{(V_{w2}/V_{w1}) - 1}{1 + G_3 + (G_2/G_1)}\right)\right). \tag{48}$$

Here, subscript "2" denotes the value at the end of the second stage of hemolysis. The ratio V_{w2}/V_{w1} can be expressed through the asphericity index of the erythrocyte, as follows:

$$\frac{V_{w2}}{V_{w1}} = \frac{V_{w0}}{V_{w1}} \cdot \frac{\delta_c - [Hb]_{c0}v_{Hb}}{1 - [Hb]_{c0}v_{Hb}}. \tag{49}$$

After sphering, the third stage of the hemolysis is started: the increase of the intracellular osmotic pressure leads to the stretching and the rupture of the erythrocyte membrane. It is known that the rupture of the membrane can be considered as a random process, where the rupture probability depends on the increased membrane tension (Evans et al., 2003; Hategan et al., 2003). Generally, the dynamics of the spontaneous decay of a subpopulation of red cells which have the same rupture probability can be

described by the following differential equation

$$\frac{\mathrm{d}}{\mathrm{d}t}n(t') = -\frac{n(t')}{\tau}, \tag{50}$$

where $n(t')$ is the number of the cells (in the subpopulation) as a function of time, $t' = t - t_2$ (i.e. time t' is counting from the beginning of the third stage), and τ is the spontaneous failure time (i.e. lifetime). The lifetime can be presented by the following function (Evans et al., 2003; Hategan et al., 2003) of the membrane tension σ:

$$\tau = \tau_0(\sigma_\beta/\sigma)^{1/2}\exp(-\sigma/\sigma_\beta), \tag{51}$$

where τ_0 a σ_β are the characteristic parameters of the red cell subpopulation. Since the cell membrane is stretching during the third stage, the osmotic pressure difference over the cell membrane is not zero (due to the increased membrane tension) and Eqs. (32) and (33) should be modified as follows:

$$\frac{V_w}{V_{w2}} = \frac{(N_{Cl}/V_{w2}) - \sum_i(z_i(\text{pH}_{in}) - z_i(\text{pH}_{in2}))C_{i2}}{[\text{NH}_4^+(ex)] \times 10^{\text{pH}_{ex}}(10^{-\text{pH}_{in}} - 10^{-\text{pH}_{in2}}) + (z_c(\text{pH}_{in}) - z_c(\text{pH}_{in2}))[\text{CO}_2(ex)]}, \tag{52}$$

$$[\text{NH}_4^+(ex)]_w \times 10^{\text{pH}_{ex}}(10^{-\text{pH}_{in}} - 10^{-\text{pH}_{in2}}) + \phi_{Hb}[\text{Hb}]_w$$
$$- \phi_{Hb2}[\text{Hb}]_{w2} + c_w(in) - c_{w2}(in) + \left(\frac{V_{w2}}{V_w} - 1\right)(2[\text{NH}_4^+(ex)]_w$$
$$- \phi_{Hb2}[\text{Hb}]_{w2} - c_{w2}(in)) + \frac{N_{Cl}}{V_{w2}}\frac{V_{w2}}{V_w} = \frac{2\sigma}{RTr}, \tag{53}$$

where N_{Cl} is the amount of Cl^- anions which were added to intracellular medium during the third stage of the hemolysis; r is the radius of the cell; R is the universal gas constant; T is the absolute temperature (in K). The membrane tension depends on the relative expansion of the membrane surface, as follows:

$$\sigma = K_S\frac{S - S_0}{S_0}, \tag{54}$$

where S_0 and S are the initial and expanded surface areas, respectively; and K_S is the membrane dilation modulus. Representing the radius and the surface area through the volume of the cell, V_c, one can rewrite Eq. (53) into the form:

$$[\text{NH}_4^+(ex)]_w \times 10^{\text{pH}_{ex}}(10^{-\text{pH}_{in}} - 10^{-\text{pH}_{in2}}) + \phi_{Hb}[\text{Hb}]_w$$
$$- \phi_{Hb2}[\text{Hb}]_{w2} + c_w(in) - c_{w2}(in) + \left(\frac{V_{w2}}{V_w} - 1\right)$$
$$\times (2[\text{NH}_4^+(ex)]_w - \phi_{Hb2}[\text{Hb}]_{w2} - c_{w2}(in))$$
$$+ \frac{N_{Cl}}{V_{w2}}\frac{V_{w2}}{V_w} = \frac{2K_S}{RTV_{c2}^{1/3}}\left(\frac{4\pi}{3}\right)^{1/3}\left(\left(\frac{V_c}{V_{c2}}\right)^{1/3} - \left(\frac{V_c}{V_{c2}}\right)^{-1/3}\right). \tag{55}$$

The volume of the cell V_c can be calculated from the water volume V_w and hemoglobin concentration $[\text{Hb}]_w$, as follows

$$V_c = V_w(1 + [\text{Hb}]_w v_{Hb}) \tag{56}$$

Assuming $\tau_0 = 3720\,\text{s}$ and $\sigma_\beta = 1.3\,\text{dyn/cm}$ (Hategan et al., 2003), estimations with Eq. (51) show that at $K_S \sim 500\,\text{dyn/cm}$ (Hochmuth and Waugh, 1987) the membrane of sphered erythrocyte is ruptured within $\sim$3 s, if the sphere volume is increased by $\sim$1%. The additional osmotic pressure which leads to such change of the spherical erythrocyte volume corresponds to $\sim$0.8 mM of additional concentration of the intracellular solutes. Therefore, one has during the third stage of hemolysis:

$$\text{pH}_{in} = \text{pH}_{in2} + \Delta\text{pH}_{in}, \quad |\Delta\text{pH}_{in}| \ll \text{pH}_{in2}, \tag{57}$$

$$V_w = V_{w2} + \Delta V_w, \quad |\Delta V_w| \ll V_{w2}. \tag{58}$$

Substituting Eqs. (56)–(58) into Eqs. (52) and (55) and taking into account that pH_{in} is changing in the range from 7 to 8, we get

$$\frac{\Delta V_w}{V_{w2}} = \frac{(2 - G_5)j_{Cl}^{in2}Bt'}{2[\text{NH}_4^+(ex)]_w(1 + G_5)6.02 \times 10^5 V_{w2}}, \tag{59}$$

$$G_5 = \frac{[\text{Hb}]_{w2}\left(\frac{23 \times 10^{\text{pH}_{in2}-6.69}}{(1 + 10^{\text{pH}_{in2}-6.69})^2} + \frac{4 \times 10^{\text{pH}_{in2}-7.89}}{(1 + 10^{\text{pH}_{in2}-7.89})^2}\right)}{[\text{NH}_4^+(ex)]_w \times 10^{\text{pH}_{ex}-\text{pH}_{in2}} - [\text{CO}_2]_w10^{\text{pH}_{in2}-6.11}}, \tag{60}$$

$$j_{Cl}^{in2} = [\text{NaHCO}_3]_w\left(-0.0541G_1 + \frac{0.198G_2}{V_{w2}/V_{w1} - 0.726}\right). \tag{61}$$

Therefore, we find that

$$\sigma = \frac{K_S B G_6 t'}{6.02 \times 10^5 V_{w2}}, \tag{62}$$

$$G_6 = \frac{(2 - G_5)j_{Cl}^{in2}}{3(1 + [\text{Hb}]_{w2}v_{Hb})[\text{NH}_4^+(ex)]_w(1 + G_5)}. \tag{63}$$

Then, using Eq. (50) the decay dynamics of the subpopulation of cells with the same parameters is

$$n(t') = n_0\exp(-\beta(t')), \tag{64}$$

n_0 and $n(t')$ are the amount of the erythrocytes in the subpopulation at the beginning and in the course of the third phase, respectively, and

$$\beta(t') = \int_0^{t'}\frac{\mathrm{d}t}{\tau(t)}. \tag{65}$$

Taking into account Eq. (62), Eq. (51) can be represented as follows:

$$\tau(t) = \tau_0(t_\beta/t)^{1/2}\exp(-t/t_\beta), \tag{66}$$

where

$$t_\beta = \frac{6.02 \times 10^5 V_{w2}\sigma_\beta}{K_S B G_6}. \tag{67}$$

Thus, during the third stage of hemolysis the number of spherical erythrocytes depends on two factors: the rate of spherical cells appearance and the rate of spherical cells decay. The probability of a spherical cell to keep its integrity (i.e. not to decay, see Eq. (64)) during a given time period after sphering is taking into account as an additional multiplicative statistical weight for the simulation of the dynamics of spherical erythrocytes distributions. We assume the parameter τ_0 has the same value of 3720 s for any erythrocyte, while the tension parameter σ_β varies from cell to cell. This consideration is assumed due to the following reason. As it was reported by Hategan et al. (2003), the parameter τ_0 is about the same for erythrocytes (~3720 s) and for giant vesicles of lipid such as SOPC (~3000 s), however, the tension parameter σ_β appears 20-fold lower for erythrocytes than for SOPC vesicles. Thus, it turned out that τ_0 is determined by the properties of the lipid bilayer rather then other components of an erythrocyte membrane, and, therefore, it does not vary from cell to cell. By the same reason, we believe the parameter τ_0 is not changed significantly for diseased erythrocytes.

3.4. Monte-Carlo approach for modeling the erythrocytes population

In spite of the relative simplicity of erythrocytes as compared to other cells, there are many biophysical parameters that must be taken into account for their characterization (e.g. volume, surface area, hemoglobin content, membrane permeability, membrane elasticity, membrane critical tension, etc.). Generally, the values of these parameters differ from cell to cell. Therefore, the distribution of these parameters plays a significant role in the understanding of many biophysical and biochemical processes within erythrocytes. Theoretically, a population of erythrocytes can be modeled by the method of histograms or the Monte-Carlo approach. We chose the Monte-Carlo approach because it is much faster, the precision of the method is not limited by the number of bins in the histograms, and the theoretical statistical error can be easily estimated (simulating a few independent random ensembles of theoretical cells) and compared with the statistical error of the experimental data (obtained by repeated experiments). Additionally, we assume a certain type of distribution functions for the cell parameters, which are used for modeling.

Applying the method of recognition of spherical erythrocytes using the scanning flow cytometer for the study of the hemolysis in isotonic NH_4Cl, we can obtain the dynamics of spherical erythrocytes distribution on such parameters as volume and hemoglobin concentration. Also, we can obtain the total amount of all erythrocytes and the fraction of spherical ones as a function of time. As it shown above, the intrinsic dynamic parameters of the model of hemolysis in isotonic NH_4Cl are t_2 and t_β. Looking at Eqs. (48) and (67) one can see, that these two intrinsic model parameters depend on two dynamic parameters of the erythrocyte: the total number of carriers B, and the ratio σ_β/K_S. Here, the term "dynamics parameters" means that these parameters can be obtained only in dynamics measurements, while other (i.e. "static") parameters can be measured separately in static experiments (e.g. native volume and hemoglobin concentration by isovolumetric sphering). It follows from the model that one cannot obtain the parameters σ_β and K_S independently, since these parameters are presented in the equations only in the form of their ratio. Thus, we chose the following list of independent individual parameters of an erythrocyte:

$$\{x_i; \quad i = 1, \ldots, 5\} = \left\{\frac{\sigma_\beta}{K_S}, B, \delta_c, V_{c0}, [Hb]_{c0}\right\}.$$

We assumed that these parameters are not correlated in an erythrocyte population, and the partial distribution of cells on each parameter is described by a log-normal distribution. This means that the overall multidimensional distribution function $F(x_1, \ldots, x_5)$ of cells is a product of one-dimensional log-normal distribution functions $L(x_i)$:

$$F(x_1, \ldots, x_5) = \prod_{i=1}^{5} L(x_i), \tag{68}$$

$$L(x_i) = \frac{1}{x_i \Omega_i \sqrt{2\pi}} \exp\left(-\frac{(\ln x_i - \ln M_i)^2}{2\Omega_i^2}\right), \tag{69}$$

where M_i and Ω_i are the parameters of the corresponding log-normal distribution function of the erythrocytes population. The goal of the study is to obtain the list of the parameters $\{M_i, \Omega_i; \quad i = 1, \ldots, 5\}$ for an erythrocytes population by interpreting the experimental data in terms of the theoretical model.

The Monte-Carlo approach was realized as follows. An ensemble of 10^5 erythrocytes with random values of their individual parameters was simulated. Then, for given values of $\{M_i, \Omega_i; \quad i = 1, \ldots, 5\}$, Eqs. (68) and (64) were used to assign a statistical weight to each erythrocyte in order to model the evolution of the erythrocytes population. Varying the values of $\{M_i, \Omega_i\}$, and using the Levenberg-Marquardt non-linear least squares algorithm a best fit to the experimental data was found for three different types of experiments: colloid osmotic lysis in isotonic solution of ammonium chloride, isovolumetric sphering in the presence of SDS, and osmotic fragility test in hypotonic external media. All three types of experiments were performed for the same population of erythrocytes, and the fitting was carried out for all experimental data simultaneously. It should be noted that we could provide this multiparameter fitting with the evolution of that many theoretical cells (10^5 erythrocytes), because a significant

acceleration of time-consuming computations of the individual parameters t_2 and t_β of each erythrocyte was achieved by applying analytical approximations of the model presented above.

4. Results and discussions

4.1. Isovolumetric sphering

Isovolumetric sphering was done to measure erythrocytes distributions for native volume and hemoglobin concentration. As soon as cells were sphered isovolumetrically, their volumes and hemoglobin concentrations were obtained from light scattering indicatrices. Figs. 3 and 4 show the obtained distributions of the erythrocytes on native volume V_{c0} and hemoglobin concentration $[Hb]_{c0}$. The distributions are approximated well by the log-normal distribution function, and the corresponding results are presented in Table 2. The values that we obtained are in good agreement with the data on mean values erythrocytes volume and hemoglobin concentration reported in the literature (Delano, 1995; Raftos et al., 1990).

4.2. Osmotic fragility test

The osmotic fragility test was done to measure erythrocyte distribution on the asphericity index. Fig. 5 shows the example (single determination) of the resulting S-shaped relation between the amount of hemolysed cells and PBS concentration. Fitting of the experimental data was done by applying the Monte-Carlo algorithm described above using distributions of native volume and hemoglobin concentration as obtained from the isovolumetric sphering procedure, and taking into account Eq. (6). The resulting parameters of the corresponding log-normal distribution for the asphericity index δ_c are presented in Table 2.

Fig. 4. Distribution of erythrocytes on hemoglobin concentration measured after isovolumetric sphering (columns—experimental histogram, line—fitting by lognormal distribution curve).

Table 2
Obtained parameters of the erythrocytes population

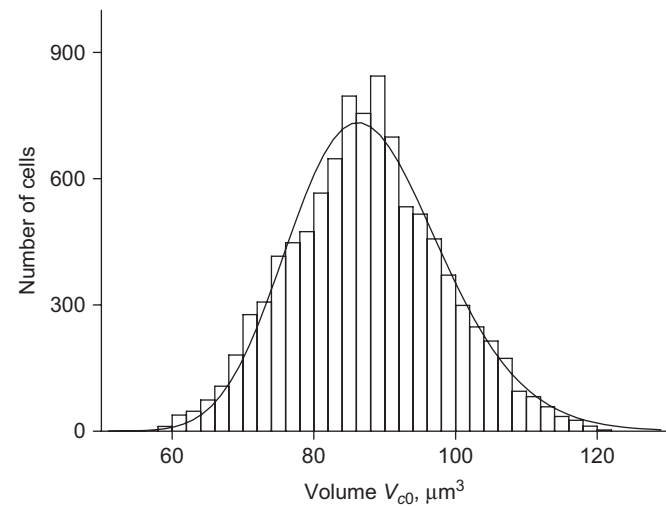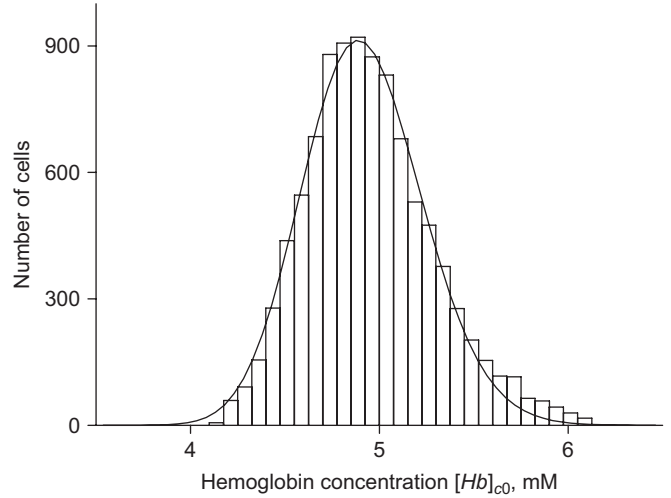|	Parameters of Lognormal distribution	
	M	Ω
V_{c0}, μm³	87.5 ± 0.3	$(1.22 \pm 0.03) \times 10^{-1}$
$[Hb]_{c0}$, mM	4.910 ± 0.005	$(6.46 \pm 0.10) \times 10^{-2}$
$V_{c0} [Hb]_{c0}$, mM μm³	430.8 ± 0.4	0.120 ± 0.001
δ_c	1.74 ± 0.02	$(4.60 \pm 0.07) \times 10^{-2}$
S, μm²	$(1.38 \pm 0.01) \times 10^2$	$(8.0 \pm 0.2) \times 10^{-2}$
B, carries	$(1.3 \pm 0.2) \times 10^6$	< 0.2
σ_β / K_S	$(1.5 \pm 0.6) \times 10^{-2}$	< 0.2

Fig. 3. Distribution of erythrocytes on volume measured after isovolumetric sphering (columns—experimental histogram, line—fitting by lognormal distribution curve).
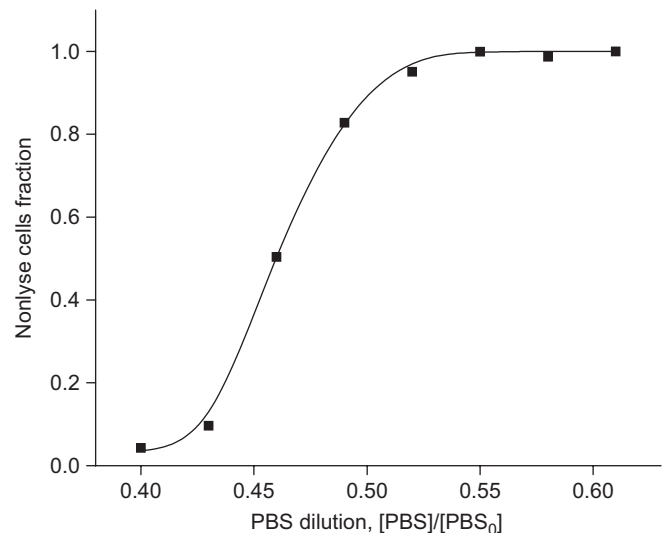

Fig. 5. Osmotic fragility test (points—experimental data, solid line—fitting curve).

The obtained values correspond to a typical values of δ_c known from the literature (Delano, 1995).

4.3. Hemolysis in isotonic solution of ammonium chloride

Hemolysis in isotonic solution of ammonium chloride was done to measure the "dynamic" parameters σ_β/K_S and B, taking account known distributions of erythrocytes on the "static" parameters V_{c0}, $[Hb]_{c0}$ and δ_c (obtained by isovolumetric sphering and the osmotic fragility test). As explained above, the five individual erythrocyte parameters σ_β/K_S, B, V_{c0}, $[Hb]_{c0}$ and δ_c determine the two intrinsic parameters t_2 and t_β of hemolysis. The distributions of these five individual parameters determine the distributions of the parameters t_2 and t_β, and, thus, the evolution of the partial distributions of sphered erythrocytes on their volume and hemoglobin concentration.

Fig. 6 shows an example of the experimental data on the Fourier parameter A_f of erythrocytes in the course of hemolysis. Taking into account theoretical calculations of A_f for swollen erythrocytes (Fig. 2), a critical value of $A_f = 0.22$ was used for recognition of spherical erythrocytes. As it follows from the experimental data (Fig. 6), erythrocytes are not decaying during a relatively long time after sphering, and $t_\beta \sim t_2$. Therefore, both dynamic parameters σ_β/K_S and B can be evaluated with reasonable precision. In order to obtain the parameters of the log-normal distributions of erythrocytes on σ_β/K_S and B, the experimental data on the amount of total erythrocytes (Fig. 7) and spherical ones (Fig. 8) as function of time, as well as the evolution of distributions of spherical erythrocytes on volume, hemoglobin concentration and hemoglobin content (Fig. 9) in the course of hemolysis were compared with corresponding theoretical calculations. The results are presented in Table 2. By fitting, we could only obtain certain values for the M_i parameters and upper limits for the Ω_i parameters of the log-normal distributions

on σ_β/K_S and B. It followed from the fitting that the parameters Ω_i of the distributions on σ_β/K_S and B are not large enough (<0.2) to have a significant effect.

The obtain number of Band 3 exchangers, B, is in good agreement with the value of 10^6 carriers/cell know from the literature (Steck, 1974). However, the ratio of characteristic stress to dilational modulus, σ_β/K_S, that represents a characteristic dilational strain of $(1.5 \pm 0.6) \times 10^{-2}$ (Table 2) appears ~5-fold higher than the ratio obtained from the numbers cited above (Hategan et al., 2003; Hochmuth and Waugh, 1987) for σ_β and K_S that yield $1.3/500 = 2.6 \times 10^{-3}$. The mismatch may be explained by experimental differences. The value of 1.3 dyn/cm (Hategan
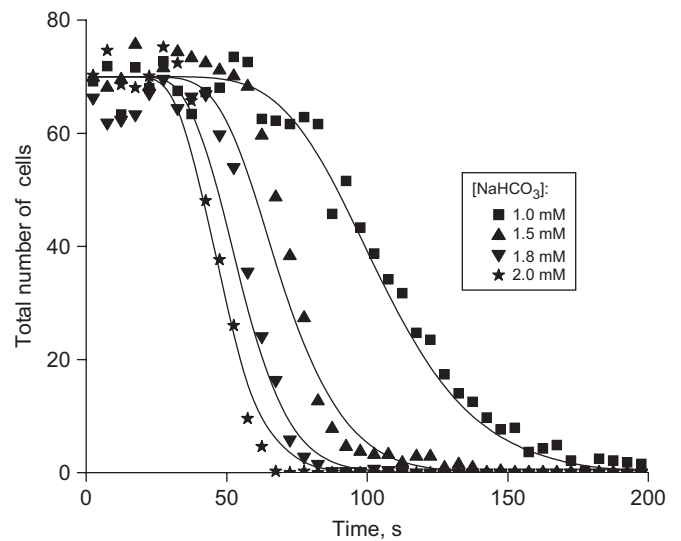
Fig. 7. Total number of erythrocytes as function of time during lysis in isotonic solution of ammonium chloride at different $NaHCO_3$ concentration (points—experimental data, solid lines—fitting curves).
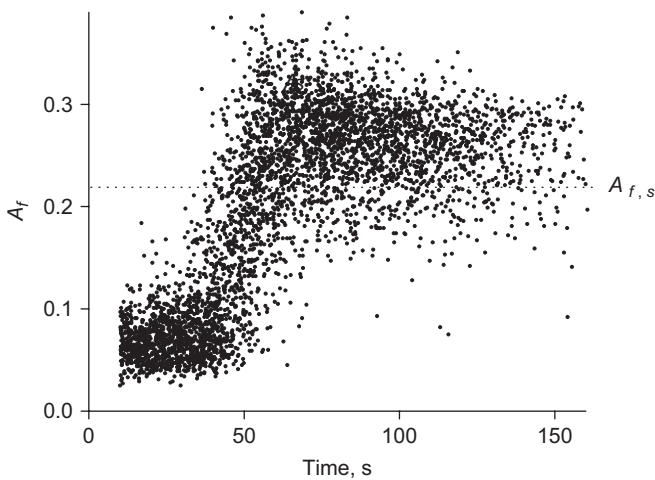
Fig. 6. Example of experimental data of the Fourier parameter A_f of erythrocytes measured in the course of hemolysis in an isotonic solution of ammonium chloride with 1 mM of $NaHCO_3$ (each point correspond to a single erythrocyte measured with the scanning flow cytometer).
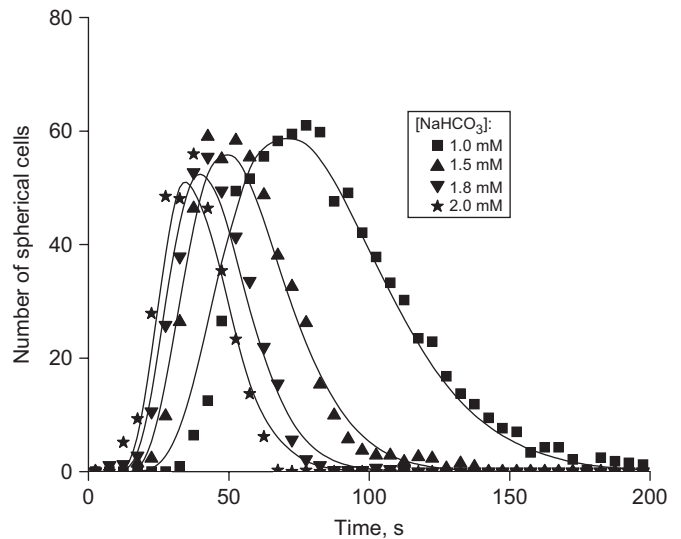
Fig. 8. Number of spherical erythrocytes as function of time during lysis in isotonic solution of ammonium chloride at different $NaHCO_3$ concentration (points—experimental results, solid lines—fitting curves).
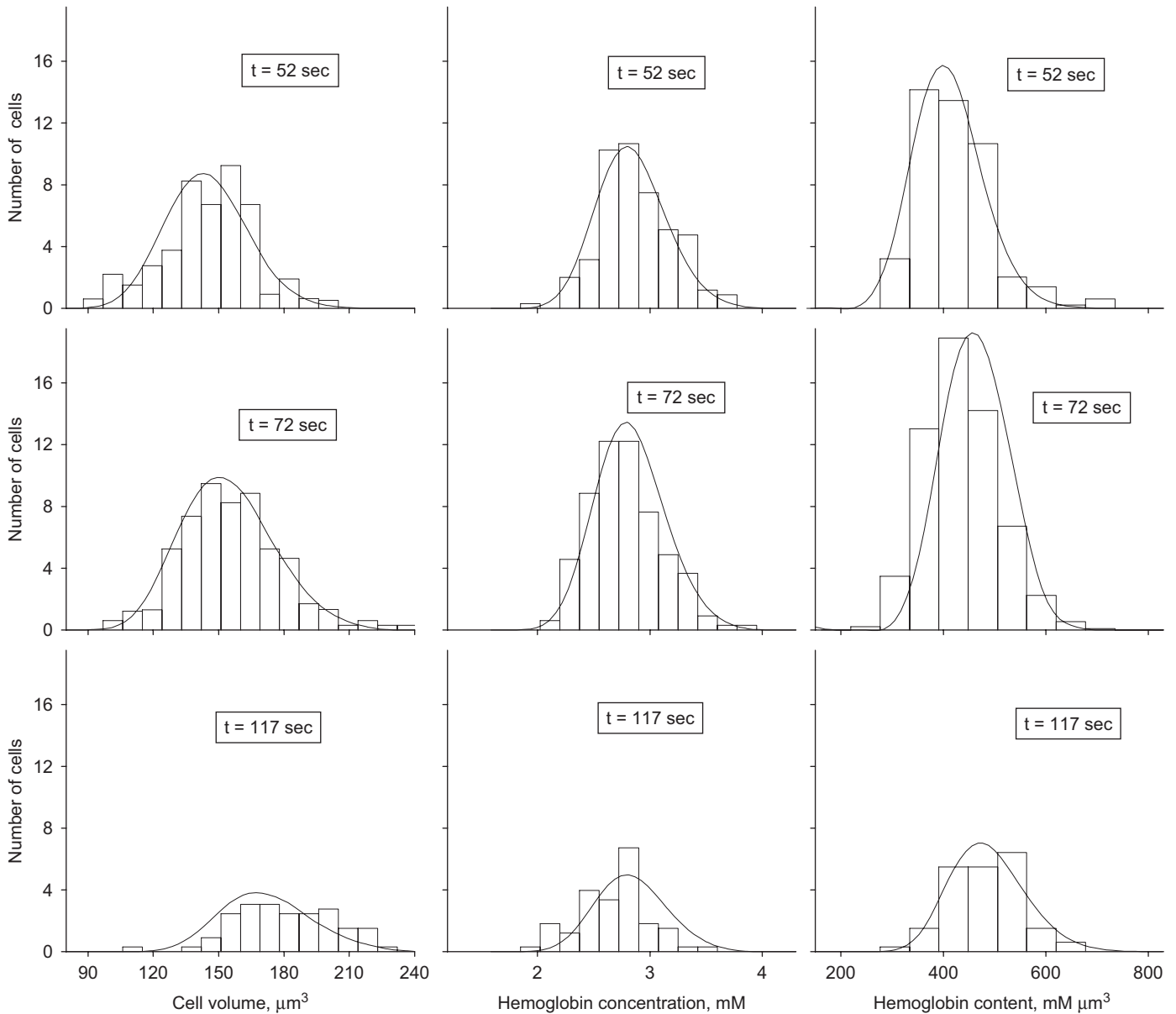
Fig. 9. Evolution of distribution of sphered erythrocytes on volume, hemoglobin concentration and hemoglobin content during hemolysis in isotonic solution of ammonium chloride with 1 mM of $NaHCO_3$ (bars—experimental results, solid line—fitting curve).

et al., 2003) for σ_β was obtained by micropipette aspiration. As the authors (Hategan et al., 2003) mentioned themselves, it is possible that the edge of a micropipette imposes a tight curvature while the cell is pressurized and the membrane tensed by aspiration. The highly curved cell membrane near the micropipette edge may lead to the cell rupture at lower aspiration pressure than the critical intracellular pressure in our experiments (without the "micropipette edge effect"). As result, we obtained higher value of the characteristic dilational strain. Another experimental difference is in the method of the sample preparation. The mechanisms responsible for erythrocyte membrane failure during phlebotomy are not clearly understood, but appeared to depend on flow-induced membrane stresses. In simple shear flows, erythrocytes

can withstand shear stress up to $1500\,dyn/cm^3$ for long duration of shear (Sutera, 1977). On other hand, cells may be damaged by a shear stress of less than $200\,dyn/cm^3$, depending on surface chemical properties and roughness and the age of the blood (Beissinger and Laugel, 1987). We checked the 2-fold increase of the sample pippeting rate did not change our experimental results significantly that indicates that the effect of the shear stress from pippeting was negligible in our experiments. Changing the flow rate of the cytometer we checked that the fluid stresses during measurements did not affect significantly our experimental results either. It should be noted that the experimental data were obtained using a single blood donor. Many erythrocyte parameters are subject to variation among individuals-both among normal populations and also in disease states,

such as thalassemia, iron deficiency, carbonic anhydrase deficiency, hereditary spherocytosis, etc. It would be interesting to test the effect of the above disease states on the hemolitic parameters that we are going to study in our future experiments.

Acknowledgments

References

Beissinger, R.L., Laugel, J.-F., 1987. Low-stress hemolysis in laminar blood flow: bulk and surface effects in capillaries. AlChE J. 33, 99–108.

Cameron, I.L., Fullerton, G.D., 1990. A model to explain the osmotic pressure behaviour of hemoglobin and serum albumin. Biochem. Cell Biol. 68, 894–898.

Delano, M.D., 1995. Simple physical constrains in hemolysis. J. Theor. Biol. 175, 517–524.

Dreybrodt, W., Lauckner, J., Liu, Z., Svensson, U., Buhmann, D., 1996. The kinetics of the reaction $CO_2 + H_2O \rightarrow H^+ + HCO_3^-$ as one of the rate limiting steps for the dissolution of calcite in the system H_2O–CO_2–$CaCO_3$. Geochim. Cosmochim. Acta, 60, 3375–3381.

Evans, E., Heinrich, V., Ludwig, F., Rawicz, W., 2003. Dynamic tension spectroscopy and strength of biomembrane. Biophys. J. 85, 2342–2350.

Faber, D.J., Aalders, M.C.G., Mik, E.G., Hooper, B.A., Gemert, M.J.C., Leeuwen, T.G., 2004. Oxygen Saturation-Dependent Absorption and Scattering of Blood. Phys. Rev. Lett. 93, 028102 (1–4).

Falke, J.J., Kanes, K.J., Chan, S.I., 1985. The kinetic equation for the chloride transport cycle of band 3. J. Biol. Chem. 260, 9545–9551.

Fisher, T.M., Haest, C.W.M., Stohr-Liesen, M., Schmid-Schodbein, H., Skalak, R., 1981. The stress-free shape of the red blood cell membrane. Biophys. J. 34, 409–422.

Freedman, J.C., Hoffman, J.F., 1979. Ionic and osmotic equilibria of human red blood cells treated with nystatin. J. Gen. Physiol. 74, 157–185.

Galanter, W.L., Hakimian, M., Labotka, R.J., 1993. Structural determinants of substrate specificity of the erythrocyte anion transporter. Am. J. Physiol. 265, C918–C926.

Gasbierg, P.K., Knauf, P.A., Brahm, J., 1996. Kinetics of bicarbonate transport in human red blood cell membranes at body temperature. J. Gen. Physiol. 108, 565–575.

Gasbjerg, P.K., Brahm, J., 1991. Kinetics of bicarbonate and chloride transport in human red cell membranes. J. Gen. Physiol. 97, 321–349.

Gunn, R.B., Dalmark, M., Tosteson, D.C., Wieth, J.O., 1973. Characteristics of chloride transport in human red blood cells. J. Gen. Physiol. 61, 185–206.

Hategan, A.P., Law, R., Kahn, S., Discher, D.E., 2003. Adhesively-tensed cell membranes: lysis kinetics and atomic force microscopy probing. Biophys. J. 85, 1–14.

Hedin, S.G., 1897. Uber die permeabilitat der Blutkorperchen. Pfuegers Arch. 68, 229.

Hochmuth, R.M., Waugh, R.E., 1987. Erythrocyte membrane elasticity and viscosity. Ann. Rev. Physiol. 49, 209–219.

Jacobs, M.H., 1924. Observation of the hemolytic actions of ammonium salts. Am. J. Physiol. 68, 134–135.

Jacobs, M.H., Stewart, D.R., 1942. The role carbonic anhydrase in certain ionic exchanges involving the erythrocytes. J. Gen. Physiol. 25, 539–552.

Joshi, A., Palsson, B.O., 1990. Metabolic dynamics in the human red cell. Part III-Metabolic reaction rates. J Theor. Biol. 142, 41–68.

Kim, Y.R., Ornstein, L., 1983. Isovolumetric sphering of erythrocytes for more accurate and precise cell volume measurement by flow cytometry. Cytometry 3, 419–427.

Klocke, R.A., 1988. Velocity of CO_2 exchange in blood. Ann. Rev. Physiol. 50, 625–637.

Knauf, P.A., Gasbierg, P.K., Brahm, J., 1996. The asymmetry of chloride transport at $38\,°C$ in human red blood cell membranes. J. Gen. Physiol. 108, 577–589.

Labotka, R.J., Lundberg, P., Kuchel, P.W., 1995. Ammonia permeability of erythrocyte membrane studied by 14N and 15N saturation transfer NMR spectroscopy. Am. J. Physiol. 268, C686–C699.

Lew, V.L., Bookchin, R.M., 1986. Volume, pH, and ion-content regulation in human red cells; analysis of transient behavior with an integrated model. J. Membr. Biol. 92, 57–74.

Liu, D., Kennedy, S.D., Knauf, P.A., 1996. Source of transport site asymmetry in the band 3 anion exchange protein determined by NMR measurements of external Cl-affinity. Biochemistry 35, 15228–15235.

Maltsev, V.P., 2000. Scanning flow cytometry for individual particle analysis. Rev. Sci. Instr. 71, 243–255.

Maltsev, V.P., Semyanov, K.A., 2004. Characterization of bio-particles from light scattering. VSP, Utrecht.

Mazeron, P., Didelon, J., Muller, S., Stoltz, J.-F., 2000. A theoretical approach of the measurement of osmotic fragility of erythrocytes by optical transmission. Photochem. Photobiol. 72, 172–178.

Mishchenko, M.I., Travis, L.D., 1994. T-matrix computations of light scattering by large spheroidal particles. Opt. Comm. 109, 16–21.

Motais, R., Guizouarn, H., Garcia-Romeu, F., 1991. Red cell volume regulation: the pivotal role of ionic strength in controlling swelling-dependent transport systems. Biochim. Biophys. Acta, 1075, 169–180.

Raftos, J.E., Bulliman, B.T., Kuchel, P.W., 1990. Evaluation of an electrochemical model of erythrocyte pH buffering using 31P nuclear magnetic resonance data. J. Gen. Physiol. 95, 1183–1204.

Saas, M.D., 1979. Effect of ammonium chloride on osmotic behaviour of red cells in nonelectrolites. Am. J. Physiol. 236, 238–243.

Semianov, K.A., Tarasov, P.A., Zharinov, A.E., Chernyshev, A.V., Hoekstra, A.G., Maltsev, V.P., 2004. Single-particle sizing from light scattering by spectral decomposition. Appl. Opt. 43, 5110–5115.

Shvalov, A.N., Soini, J.T., Chernyshev, A.V., Tarasov, P.A., Soini, E., Maltsev, V.P., 1999. Light-scattering properties of individual erythrocytes. Appl. Opt. 38, 230–235.

Shvalov, A.N., Soini, J.T., Surovtsev, I.V., Kochneva, G.V., Sivolobova, G.F., Petrov, A.K., Maltsev, V.P., 2000. Individual Escherichia coli cells studied from light scattering with the scanning flow cytometer. Cytometry 41, 41–45.

Steck, T., 1974. The organization of proteins in the human red blood cell membrane. J. Cell Biol. 62, 1–19.

Sutera, S.P., 1977. Flow-induced trauma to blood cells. Circ. Res. 41, 2–8.

Werner, A., Heinrich, R., 1985. A kinetic model for the interaction of energy methabolism and osmotic states of human erythrocytes. Analysis of the stationary "in vivo" state and of time dependent variations under blood preservation conditions. Biomed. Biochem. Acta, 44, 185–212.

Widdas, W.F., Baker, G.F., 1998. The physiological properties of human red cells as derived from kinetics osmotic volume changes. Cytobios 95, 173–210.